

Electromagnetic and hadronic decay of fully heavy tetraquarks

Wen-Long Sang,^{1,*} Tao Wang,¹ Yu-Dong Zhang^{2,†} and Feng Feng^{3,4,‡}

¹*School of Physical Science and Technology, Southwest University, Chongqing 400700, China*

²*Institute of Particle Physics and Key Laboratory of Quark and Lepton Physics (MOE), Central China Normal University, Wuhan, Hubei 430079, China*

³*China University of Mining and Technology, Beijing 100083, China*

⁴*Institute of High Energy Physics, Chinese Academy of Sciences, Beijing 100049, China*



(Received 16 December 2023; accepted 21 February 2024; published 13 March 2024)

In this study, we compute the electromagnetic and hadronic decay widths of the S-wave fully heavy tetraquark T_{4Q} ($Q = c$ or b) at lowest order in α_s and v , in the framework of nonrelativistic QCD. The short-distance coefficients are determined through the standard procedure of matching. The nonperturbative long-distance matrix elements are related to the phenomenological four-body Schrödinger wave functions at the origin, whose values are taken from literature. The branching fractions are predicted to be around 10^{-3} and 10^{-6} for the T_{4c} hadronic decay and electromagnetic decay, respectively. Combining our results with the T_{4c} production cross sections at the LHC, we also predict the event numbers for various decay channels. With integrated luminosity $\mathcal{L} = 100 \text{ fb}^{-1}$, it is expected that the event numbers can reach 10^3 – 10^4 for $T_{4c} \rightarrow \gamma\gamma$, and 10^5 – 10^6 for $T_{4c} \rightarrow \text{LH}$, at the LHC. The detecting prospect is promising. In addition, the decay widths of T_{4b} are estimated based on simple dimensional analysis as well as velocity scaling rule.

DOI: [10.1103/PhysRevD.109.056016](https://doi.org/10.1103/PhysRevD.109.056016)

I. INTRODUCTION

Searching for exotic states is full of challenges and opportunities. Compared with conventional hadrons, exotic states may provide a better environment to reveal the nonperturbative nature of QCD. In 2020, the LHCb Collaboration reported a narrow resonance around 6.9 GeV with the significance larger than 5σ , dubbed as $X(6900)$, a broad structure with the mass ranging from 6.2 GeV to 6.8 GeV, and a hint for another structure around 7.2 GeV in the $di-J/\psi$ invariant mass spectrum [1]. The narrow structure contains at least $cc\bar{c}\bar{c}$ configuration and therefore is naturally considered as a fully charmed tetraquark. By assuming that the nonresonant single-parton scattering (NRSPS) continuum is not disturbed, the mass and width of $X(6900)$ are determined to be $M = 6905 \pm 11 \pm 7 \text{ MeV}$ and $\Gamma = 80 \pm 19 \pm 33 \text{ MeV}$, respectively, while, they become $M = 6886 \pm 11 \pm 11 \text{ MeV}$ and

$\Gamma = 168 \pm 33 \pm 69 \text{ MeV}$ when assuming the NRSPS continuum interferes with a broad structure above the $di-J/\psi$ mass threshold.

Soon afterward the $X(6900)$ was confirmed in the $di-J/\psi$ channel by the CMS Collaboration [2–4], and the $di-J/\psi$ as well as $J/\psi\psi(2S)$ channels by the ATLAS Collaboration [5], respectively. For CMS, the mass and width are determined to be $M = 6927 \pm 9 \pm 4 \text{ MeV}$, $\Gamma = 122^{+24}_{-21} \pm 18 \text{ MeV}$, or $M = 6847^{+44+48}_{-28-20} \text{ MeV}$ and $\Gamma = 191^{+66+25}_{-49-17} \text{ MeV}$ when considering or not considering the interferences among resonances, respectively [3]. For ATLAS, the mass and decay width are $6.87 \pm 0.03^{+0.06}_{-0.01} \text{ GeV}$ and $0.12 \pm 0.04^{+0.03}_{-0.01} \text{ GeV}$, respectively [5]. Moreover, some new resonances are observed, i.e., $X(6600)$ and $X(7200)$ by CMS [2–4], and $X(6200)$, $X(6600)$, and $X(7200)$ by ATLAS [6]. On the other hand, in the bottom quark sector, an observation of a Υ pair was reported by the CMS Collaboration [7]; however the structure was not yet confirmed by the later analysis from CMS [8]. In addition, the LHCb Collaboration studied the $\Upsilon\mu^+\mu^-$ invariant mass spectrum; however no reliable signals were observed [9].

On the theoretical side, the explorations on fully heavy tetraquark date back to the 1970s [10–12]. The discovery of $X(6900)$ in experiment has inspired extensive theoretical investigations. Various approaches are adopted to

*wlsang@swu.edu.cn

†ydzhang@mails.ccnu.edu.cn

‡f.feng@outlook.com

Published by the American Physical Society under the terms of the [Creative Commons Attribution 4.0 International license](https://creativecommons.org/licenses/by/4.0/). Further distribution of this work must maintain attribution to the author(s) and the published article's title, journal citation, and DOI. Funded by SCOAP³.

understand the nature of these fully charmed tetraquarks, e.g., constituent quark models [13–23], QCD sum rules [24–27], diffusion Monte Carlo [28,29], lattice [30], partial wave analysis [31], and color evaporation model [32,33]. Albeit many theoretical researches on these fully charmed tetraquark states are performed, the interpretations for them are still controversial. Many interpretations exist in literature, such as P-wave tetraquark [34,35], radial excitation [26,36,37], $\bar{\chi}_{c0}\chi_{c0}$ molecular state [38], hybrid state [39], and resonance formed in charmonium-charmonium scattering or kinematic cusp arising from final-state interaction [40,41]. For more references, we refer the reader to Ref. [42] and references therein.

While the spectra have been widely studied, the decay property and production mechanism of the fully heavy tetraquarks are relatively less investigated, particularly based on model independent methods. In Ref. [43], a factorization formula for S-wave T_{4c} inclusive production is presented in the framework of nonrelativistic QCD (NRQCD) [44] (a similar idea can be also found in [45,46]). A key observation is that, prior to hadronization, two charm quarks and two anticharm quarks have to be created at a rather short distance $< 1/m_c$; thus one can invoke asymptotic freedom to factorize the production rate as the product of the perturbative calculable short-distance part and the nonperturbative long-distance part. By employing this factorization formula, the T_{4c} production at the LHC was studied in Refs. [43,47], and production at the B factory was investigated in Refs. [48,49]. Analogous to the case in the quarkonium sector, one anticipates that the NRQCD factorization ansatz should hold for the fully heavy tetraquark inclusive and electromagnetic decay. This work aims to compute the decay widths for $T_{4Q} \rightarrow \gamma\gamma$ and $T_{4Q} \rightarrow \text{LH}$, where LH denotes the light hadrons. Note that, by assigning T_{4Q} to be an S-wave tetraquark, the feasible J^{PC} quantum number of T_{4Q} can be 0^{++} , 1^{+-} and 2^{++} .

The paper is organized as follows. In Sec. II, we present the factorization formulas for T_{4Q} hadronic and electromagnetic decay, and sketch the procedure to match the short-distance coefficient (SDC). In Sec. III, we describe the computing techniques, and present the analytic expressions for the SDCs. Section IV is devoted to phenomenological predictions and discussions. We make a summary in Sec. V.

II. THEORETICAL FRAMEWORK

A. NRQCD factorization for T_{4Q} decay

In Ref. [43], the NRQCD factorization formula for T_{4Q} inclusive production was proposed. It is straightforward to convert the factorization formula into that for the T_{4Q} electromagnetic and hadronic decay. Specifically, we can

express the decay widths of $T_{4Q} \rightarrow \text{LH}$ at the lowest order in velocity as follows¹:

$$\Gamma[T_{4Q}^{0^{++}} \rightarrow \text{LH}] = c_{\text{LH},1}^{(0)} \times \frac{2m_H \langle \mathcal{O}_{\bar{6}\bar{6}\bar{6}}^{(0)} \rangle}{4^2 (2m_Q)^4} + c_{\text{LH},2}^{(0)} \times \frac{2m_H \langle \mathcal{O}_{\bar{3}\bar{3}\bar{3}}^{(0)} \rangle}{4^2 (2m_Q)^4} + c_{\text{LH},3}^{(0)} \times \frac{2m_H \langle \mathcal{O}_{\text{mixing}}^{(0)} \rangle}{4^2 (2m_Q)^4}, \quad (1a)$$

$$\Gamma[T_{4Q}^{2^{++}} \rightarrow \text{LH}] = c_{\text{LH}}^{(2)} \times \frac{2m_H \langle \mathcal{O}_{\bar{3}\bar{3}\bar{3}}^{(2)} \rangle}{4^2 (2m_Q)^4}, \quad (1b)$$

where the superscript in T_{4Q} denotes the quantum number J^{PC} of the T_{4Q} , m_Q and m_H signify the masses of the heavy quark Q and the T_{4Q} respectively, and c represent the SDCs.

The long-distance matrix elements (LDMEs) in (1) are defined via

$$\langle \mathcal{O}_{\bar{6}\bar{6}\bar{6}}^{(0)} \rangle = |\langle 0 | \mathcal{O}_{\bar{6}\bar{6}\bar{6}}^{(0)} | T_{4Q} \rangle|^2, \quad (2a)$$

$$\langle \mathcal{O}_{\bar{3}\bar{3}\bar{3}}^{(J)} \rangle = |\langle 0 | \mathcal{O}_{\bar{3}\bar{3}\bar{3}}^{(J)} | T_{4Q} \rangle|^2, \quad (2b)$$

$$\langle \mathcal{O}_{\text{mixing}}^{(0)} \rangle = \text{Re}[\langle 0 | \mathcal{O}_{\bar{3}\bar{3}\bar{3}}^{(0)} | T_{4Q} \rangle \langle T_{4Q} | \mathcal{O}_{\bar{6}\bar{6}\bar{6}}^{(0)\dagger} | 0 \rangle], \quad (2c)$$

where $J = 0, 2$, and the T_{4Q} state is nonrelativistically normalized. Note that, in Eq. (2), we have made use of the “vacuum-saturation approximation” to transfer the hadronic matrix elements into the electromagnetic matrix elements [44]. The operators in (2) are constructed in the diquark antidiquark basis,² where the spin configuration and color configuration of the diquark are correlated due to Fermi statistics. Specifically, the S-wave spin-singlet diquark must be a color sextet, while the S-wave spin-triplet diquark must be a color triplet. Explicitly, these operators read as

¹Owing to the Landau-Yang theorem, the $T_{4Q}^{1^{+-}}$ into double photons or double gluons is strictly forbidden. Moreover, $T_{4Q}^{0^{++}}$ or $T_{4Q}^{1^{+-}}$ decaying into a pair of light quarks is also forbidden according to the helicity conservation of light quark and the angular momentum conservation. The $T_{4Q}^{1^{+-}}$ can decay into triple gluons or a gluon associated with a pair of light quarks, which however is suppressed by the strong coupling constant α_s . Thus, we will not consider the decay of $T_{4Q}^{1^{+-}}$ in the current work.

²Alternatively, the NRQCD operators can be constructed in $Q\bar{Q}-Q\bar{Q}$ basis, as done in Ref. [46], where the $Q\bar{Q}$ cluster can be either in color singlet or color octet. Actually, the NRQCD operators in Eq. (3) can be converted to the operators in Ref. [46] by Fierz transformation.

$$\mathcal{O}_{\mathbf{6}\mathbf{\bar{6}}}^{(0)} = [\psi_a^T(i\sigma^2)\psi_b][\chi_c^\dagger(i\sigma^2)\chi_d^*]C_{\mathbf{6}\mathbf{\bar{6}}}^{ab;cd}, \quad (3a)$$

$$\mathcal{O}_{\mathbf{3}\mathbf{\bar{3}}}^{(0)} = -\frac{1}{\sqrt{3}}[\psi_a^T(i\sigma^2)\sigma^i\psi_b][\chi_c^\dagger(i\sigma^2)\chi_d^*]C_{\mathbf{3}\mathbf{\bar{3}}}^{ab;cd}, \quad (3b)$$

$$\mathcal{O}_{\mathbf{3}\mathbf{\bar{3}}}^{(2)} = \frac{1}{2}\Gamma^{ij,kl}\epsilon_H^{ij*}[\psi_a^T(i\sigma^2)\sigma^k\psi_b][\chi_c^\dagger(i\sigma^2)\chi_d^*]C_{\mathbf{3}\mathbf{\bar{3}}}^{ab;cd}, \quad (3c)$$

where ψ and χ^\dagger are Pauli spinor fields that annihilate the heavy quark and antiquark, respectively, σ^i denotes the Pauli matrix, and ϵ_H denotes the polarization tensor of the $T_{4Q}^{2^{++}}$. The Latin letters $i, j, k = 1, 2, 3$ signify the Cartesian indices, whereas $a, b, c, d = 1, 2, 3$ denote the color indices. The symmetric traceless tensor is

$$\Gamma^{ij,kl} = \delta^{ik}\delta^{jl} + \delta^{il}\delta^{jk} - \frac{2}{3}\delta^{ij}\delta^{kl}. \quad (4)$$

The color projection tensors in (3) are given by

$$C_{\mathbf{6}\mathbf{\bar{6}}}^{ab;cd} \equiv \frac{1}{2\sqrt{6}}(\delta^{ac}\delta^{bd} + \delta^{ad}\delta^{bc}), \quad (5a)$$

$$C_{\mathbf{3}\mathbf{\bar{3}}}^{ab;cd} \equiv \frac{1}{2\sqrt{3}}(\delta^{ac}\delta^{bd} - \delta^{ad}\delta^{bc}). \quad (5b)$$

It is straightforward to convert the factorization formula (1) into that for $T_{4Q} \rightarrow \gamma\gamma$. Correspondingly, we replace the subscript LH with $\gamma\gamma$ in the SDCs to denote the SDCs for $T_{4Q} \rightarrow \gamma\gamma$.

B. Procedure to determine the SDCs

With the spirit of factorization, the SDCs in (1) are insensitive to the hadronization effects in the tetraquark; thus they can be deduced with the aid of the standard perturbative matching techniques, that is, by replacing the physical T_{4Q} state in (1) with a fictitious “tetraquark” state composed of a pair of heavy quarks and a pair of heavy antiquarks, carrying the same quantum number as the physical T_{4Q} . Conveniently, we label the fictitious state with \tilde{T}_{4Q} . After this replacement, we can compute both sides of (1) order by order in α_s ; thus the SDCs can be solved at desired order of α_s .

To calculate the left-hand side of (1), we first write down the amplitude of the free $QQ\bar{Q}\bar{Q}$ decay, then enforce the $QQ\bar{Q}\bar{Q}$ in the desired spin, total angular momentum, and color quantum numbers. In a shortcut, we employ the spin-singlet projector Π_0 and spin-triplet projector Π_1 to enforce the diquark in $S = 0$ and $S = 1$ respectively, and we make use of the color projectors $C_{\mathbf{6}\mathbf{\bar{6}}}^{ab;cd}$ and $C_{\mathbf{3}\mathbf{\bar{3}}}^{ab;cd}$ to extract the color-sextet and color-triplet parts of the diquark, respectively. For the case of the diquark and antiquark in the spin-triplet configuration, we apply the covariant projectors to pick out the total angular momentum number of \tilde{T}_{4Q} .

Concretely, we ensure the $QQ\bar{Q}\bar{Q}$ in $J^{PC} = 0^{++}$ through the replacement

$$u_i^a u_j^b \bar{v}_k^c \bar{v}_l^d \rightarrow (C\Pi_0)^{ij}(\Pi_0 C)^{lk}C_{\mathbf{6}\mathbf{\bar{6}}}^{ab;cd}, \quad (6)$$

for the spin-singlet diquark configuration, and ensure the $QQ\bar{Q}\bar{Q}$ in $J^{PC} = 0^{++}, 2^{++}$ through the replacement

$$u_i^a u_j^b \bar{v}_k^c \bar{v}_l^d \rightarrow (C\Pi_{1\mu})^{ij}(\Pi_{1\nu} C)^{lk}C_{\mathbf{3}\mathbf{\bar{3}}}^{ab;cd}J_{0,2}^{\mu\nu}, \quad (7)$$

for the spin-triplet diquark configuration, where u and v denote the Dirac spinors of heavy quarks. In (6) and (7), the spin projectors are

$$\Pi_0 = \frac{(\not{P} - m_Q)\gamma_5}{\sqrt{2}}, \quad (8a)$$

$$\Pi_1^\mu = \frac{(\not{P} - m_Q)\gamma^\mu}{\sqrt{2}}, \quad (8b)$$

and the covariant projectors $J_{0,2}^{\mu\nu}$ are

$$J_0^{\mu\nu} = \frac{1}{\sqrt{3}}\eta^{\mu\nu}, \quad (9a)$$

$$J_2^{\mu\nu} = \epsilon_{H,\alpha\beta} \left[\frac{1}{2}\eta^{\mu\alpha}\eta^{\nu\beta} + \frac{1}{2}\eta^{\mu\beta}\eta^{\nu\alpha} - \frac{1}{3}\eta^{\mu\nu}\eta^{\alpha\beta} \right], \quad (9b)$$

where P denotes the momentum of the T_{4Q} , and $\eta^{\mu\nu} \equiv -g^{\mu\nu} + \frac{P^\mu P^\nu}{P^2}$.

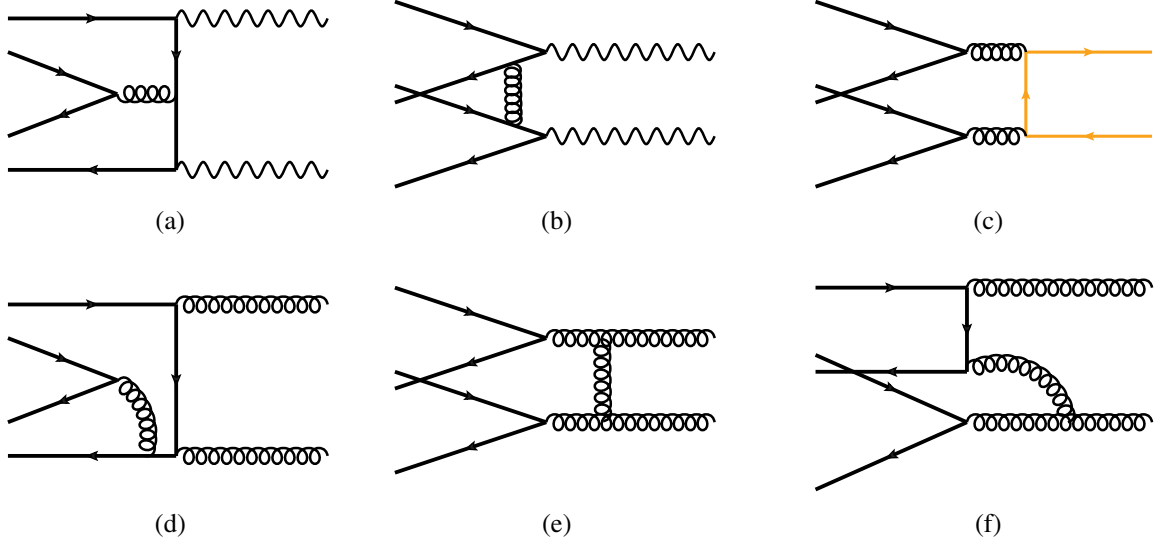
Furthermore, the squared amplitude can be obtained by multiplying the amplitude with its complex conjugate, summing the polarizations of the final states, and averaging the polarizations of the \tilde{T}_{4Q} . It is worth noting that, in order to match $c_{\gamma\gamma,3}^{(0)}$ and $c_{\text{LH},3}^{(0)}$, the SDCs of the mixing LDME $\langle \mathcal{O}_{\text{mixing}}^{(0)} \rangle$, one must utilize the replacement (7) for the quark-level amplitude, and the replacement (6) for the complex conjugate of the amplitude.

For the sake of completeness, we present the results for the perturbative LDMEs that involve \tilde{T}_{4Q} :

$$\begin{aligned} |\langle 0 | \mathcal{O}_{\mathbf{6}\mathbf{\bar{6}}}^{(0)} | \tilde{T}_{4Q} \rangle|^2 &= |\langle 0 | \mathcal{O}_{\mathbf{3}\mathbf{\bar{3}}}^{(J)} | \tilde{T}_{4Q} \rangle|^2 \\ &= \text{Re}[\langle 0 | \mathcal{O}_{\mathbf{3}\mathbf{\bar{3}}}^{(0)} | \tilde{T}_{4Q} \rangle \langle \tilde{T}_{4Q} | \mathcal{O}_{\mathbf{6}\mathbf{\bar{6}}}^{(0)\dagger} | 0 \rangle] \\ &= 4^2(2m_Q)^4, \end{aligned} \quad (10)$$

where the heavy quark states are relativistically normalized, which is consistent with the convention adopted for the spin projectors (8).

Now, we collect all the essential ingredients to evaluate the SDCs.

FIG. 1. Some representative Feynman diagrams for $T_{4Q} \rightarrow \gamma\gamma$, $T_{4Q} \rightarrow q\bar{q}$, and $T_{4Q} \rightarrow gg$.

III. ANALYTIC EXPRESSIONS FOR THE SDCs

We use the package FEYNARTS [50] to generate quark-level Feynman diagrams and the corresponding amplitudes. There are 40, 4, and 62 nonvanishing Feynman diagrams for $T_{4Q} \rightarrow \gamma\gamma$, $T_{4Q} \rightarrow q\bar{q}$, and $T_{4Q} \rightarrow gg$, respectively. Some representative diagrams are illustrated in Fig. 1. After implementing the replacements (6) and (7) to ensure $QQ\bar{Q}\bar{Q}$ in the correct quantum numbers, we use the packages FEYNCALC [51] and FORMLINK [52,53] to conduct the trace over Dirac and $SU(N_c)$ color matrices, and the contraction over Lorentz indices.

Following the matching procedure sketched in Sec. II, it is straightforward to deduce the SDCs:

$$c_{\gamma\gamma,1}^{(0)} = \frac{128\pi^3 e_Q^4 \alpha^2 \alpha_s^2}{3m_H m_Q^4}, \quad (11a)$$

$$c_{\gamma\gamma,2}^{(0)} = \frac{2304\pi^3 e_Q^4 \alpha^2 \alpha_s^2}{m_H m_Q^4}, \quad (11b)$$

$$c_{\gamma\gamma,3}^{(0)} = \frac{256\sqrt{6}\pi^3 e_Q^4 \alpha^2 \alpha_s^2}{m_H m_Q^4}, \quad (11c)$$

$$c_{\gamma\gamma}^{(2)} = \frac{16384\pi^3 e_Q^4 \alpha^2 \alpha_s^2}{15m_H m_Q^4}, \quad (11d)$$

for $T_{4Q} \rightarrow \gamma\gamma$, and

$$c_{\text{LH},1}^{(0)} = \frac{484\pi^3 \alpha_s^4}{27m_H m_Q^4}, \quad (12a)$$

$$c_{\text{LH},2}^{(0)} = \frac{72\pi^3 \alpha_s^4}{m_H m_Q^4}, \quad (12b)$$

$$c_{\text{LH},3}^{(0)} = \frac{88\sqrt{6}\pi^3 \alpha_s^4}{3m_H m_Q^4}, \quad (12c)$$

$$c_{\text{LH}}^{(2)} = \frac{6272\pi^3 \alpha_s^4}{135m_H m_Q^4} \left(1 + \frac{48}{49}n_L\right), \quad (12d)$$

for $T_{4Q} \rightarrow \text{LH}$, where $n_L = 3$ represents the number of light quark flavors. Note that the n_L term in $c_{\text{LH}}^{(2)}$ corresponds to the contribution from $T_{4Q} \rightarrow q\bar{q}$. It is worth emphasizing that the m_H in the SDCs, originating from the prefactor of the formula of decay width, cancels the same factor in (1); thus the final decay widths are free of the m_H .

IV. PHENOMENOLOGICAL PREDICTIONS

Prior to making phenomenological predictions, we need to fix the various input parameters.³We take the charm quark mass to be $m_c = 1.5$ GeV. We take the fine structure coupling constant $\alpha = 1/137$. The QCD running coupling constant at $\mu_R = 2m_c$ is evaluated with the aid of the package RunDec [54]. We have varied μ_R from m_c to $4m_c$ to estimate the theoretical uncertainty.

We should further choose the NRQCD LDMEs. These nonperturbative LDMEs can be related to the phenomenological four-body Schrödinger wave functions at the origin [47]:

³Since exact values of the LDMEs of T_{4b} are currently absent in the literature, in this section, we are mainly concerned with predictions for T_{4c} , and briefly estimate the decay widths for T_{4b} .

TABLE I. Numerical values of the LDMEs for T_{4c} in Model I [22] and Model II [35], in unit of GeV⁹.

J^{PC}	0^{++}			1^{+-}	2^{++}
LDMEs	$\langle \mathcal{O}_{\mathbf{3}\otimes\mathbf{3}}^{(0)} \rangle$	$\langle \mathcal{O}_{\text{mixing}}^{(0)} \rangle$	$\langle \mathcal{O}_{\mathbf{6}\otimes\mathbf{6}}^{(0)} \rangle$	$\langle \mathcal{O}_{\mathbf{3}\otimes\mathbf{3}}^{(1)} \rangle$	$\langle \mathcal{O}_{\mathbf{3}\otimes\mathbf{3}}^{(2)} \rangle$
Model I	0.0347	0.0211	0.0128	0.0260	0.0144
Model II	0.0187	-0.0161	0.0139	0.0160	0.0126

$$\langle \mathcal{O}_{\mathbf{3}\otimes\mathbf{3}}^{(J)} \rangle \approx 16\psi_3^{(J)}(0)\psi_3^{(J)*}(0), \quad (13a)$$

$$\langle \mathcal{O}_{\mathbf{6}\otimes\mathbf{6}}^{(0)} \rangle \approx 16\psi_6(0)\psi_6^*(0), \quad (13b)$$

$$\langle \mathcal{O}_{\text{mixing}}^{(0)} \rangle \approx 16|\psi_3^{(0)}(0)\psi_6^*(0)|. \quad (13c)$$

In this work, we adopt two phenomenological models to evaluate the LDMEs [22,35]. In both models, Cornell-type potentials with spin-dependent corrections are assumed, and the Gaussian basis method is utilized to solve for the four-body tetraquark wave functions. However unlike Model I [22], which is based on a nonrelativistic quark model, there involves a relativistic kinetic term in Model II [35]. We enumerate the values of the LDMEs for T_{4c} in Table I. Note that there is a sign difference for the value of $\langle \mathcal{O}_{\text{mixing}}^{(0)} \rangle$ from the two models.

If assuming T_{4c} decay is saturated by its decay into double J/ψ , we can approximate the total decay width of T_{4c} through

$$\Gamma_{\text{total}}(T_{4c}) \approx \Gamma[T_{4c} \rightarrow J/\psi J/\psi] \approx 0.12 \text{ GeV}, \quad (14)$$

where 0.12 GeV corresponds to the central value of the decay width determined by the ATLAS Collaboration [6], and is roughly the average of the two fitting values from the LHCb measurement [1]. This value is also consistent with the no-interference fitting value by the CMS Collaboration [3].

Now, we collect all ingredients to make phenomenological predictions. The theoretical results of the decay widths as well as the corresponding branching fractions for $T_{4c} \rightarrow \gamma\gamma$ and $T_{4c} \rightarrow \text{LH}$ are tabulated in Table II. We observe that, the branching fractions for $T_{4c} \rightarrow \text{LH}$ are about 3 orders of magnitude larger than these for $T_{4c} \rightarrow \gamma\gamma$, which is attributed to enhancement from the strong coupling constant, i.e., $\alpha_s^2/\alpha^2 \approx 10^3$. By comparing the predictions from the two phenomenological models, we find the theoretical results for 2^{++} tetraquark are insensitive to the models, while the predictions for 0^{++} from Model I are more than 2 times larger than from Model II. As can be seen from Table I, the values of $\langle \mathcal{O}_{\text{mixing}}^{(0)} \rangle$ in the two models take different signs. Therefore, the interfering term is constructive in Model I, while destructive in Model II, which explains why the branching fractions for 0^{++} from Model I are larger. Finally, it is worth noting that our prediction for the $\text{Br}[T_{4c}^{0^{++}} \rightarrow \gamma\gamma]$ is roughly consistent with the value $(2.77 \pm 0.36) \times 10^{-6}$ estimated based on the vector meson dominance [55].

To evaluate the numerical values for T_{4b} decay, we should determine the LDMEs. The exact values of the LDMEs for T_{4b} are absent in the literature. As a very crude estimate [47], we temporarily assume that T_{4Q} is comprised of a compact diquark-antidiquark cluster, each of which is bound by attractive color Coulomb forces. One then estimates the ratio of the four-body Schrödinger wave functions at the origin for T_{4c} and for T_{4b} through simple dimensional analysis. Hence, we may roughly estimate the LDMEs of the T_{4b} by

$$\begin{aligned} \langle \mathcal{O}^{(J)} \rangle_{T_{4b}} &= \langle \mathcal{O}^{(J)} \rangle_{T_{4c}} \times \frac{\langle \mathcal{O} \rangle_{T_{4b}, \text{Coulomb}}}{\langle \mathcal{O} \rangle_{T_{4c}, \text{Coulomb}}} \\ &\approx \langle \mathcal{O}^{(J)} \rangle_{T_{4c}} \times \left(\frac{m_b \alpha_s^b}{m_c \alpha_s^c} \right)^9, \end{aligned} \quad (15)$$

where α_s^Q represents the strong coupling $\alpha_s(m_Q v_Q) \sim v_Q$, v_Q stands for the typical velocity of the heavy quark

TABLE II. Theoretical predictions on the decay widths and branching fractions. We estimate the uncertainty by sliding μ_R from m_c to $4m_c$.

$m_c = 1.5 \text{ GeV}; \Gamma(\times 10^{-1} \text{ MeV})$				
Channel	Model I		Model II	
	Γ_{LO}	Br	Γ_{LO}	Br
$T_{4c}^{0^{++}} \rightarrow \gamma\gamma$	$5.17^{+3.29}_{-1.64} \times 10^{-3}$	$4.31^{+2.74}_{-1.37} \times 10^{-6}$	$1.85^{+1.18}_{-0.59} \times 10^{-3}$	$1.54^{+0.98}_{-0.49} \times 10^{-6}$
$T_{4c}^{2^{++}} \rightarrow \gamma\gamma$	$0.87^{+0.55}_{-0.28} \times 10^{-3}$	$0.72^{+0.46}_{-0.23} \times 10^{-6}$	$0.76^{+0.48}_{-0.24} \times 10^{-3}$	$0.63^{+0.40}_{-0.20} \times 10^{-6}$
$T_{4c}^{0^{++}} \rightarrow \text{LH}$	$1.23^{+2.07}_{-0.66}$	$1.03^{+1.72}_{-0.55} \times 10^{-3}$	$0.13^{+0.21}_{-0.07}$	$0.11^{+0.18}_{-0.06} \times 10^{-3}$
$T_{4c}^{2^{++}} \rightarrow \text{LH}$	$0.77^{+1.28}_{-0.41}$	$0.64^{+1.07}_{-0.34} \times 10^{-3}$	$0.67^{+1.12}_{-0.36}$	$0.56^{+0.94}_{-0.30} \times 10^{-3}$

TABLE III. Estimation on the event yields at the LHC, where the T_{4c} production cross sections at the LHC σ_{LHC} are taken from Ref. [47] and the integrated luminosity $\mathcal{L} = 100 \text{ fb}^{-1}$ is chosen. The two uncertainties in N_{events} are transferred from the uncertainties in the cross sections and branching fractions, respectively.

Channel	Model I		Model II	
	$\sigma_{\text{LHC}} \text{ [nb]}$	N_{events}	$\sigma_{\text{LHC}} \text{ [nb]}$	N_{events}
$T_{4c}^{0^{++}} \rightarrow \gamma\gamma$	37 ± 26	$(1.59 \pm 1.12^{+1.01}_{-0.51}) \times 10^4$	9 ± 6	$(1.39 \pm 0.93^{+0.88}_{-0.44}) \times 10^3$
$T_{4c}^{2^{++}} \rightarrow \gamma\gamma$	93 ± 65	$(6.72 \pm 4.70^{+4.27}_{-2.13}) \times 10^3$	81 ± 57	$(5.12 \pm 3.61^{+3.26}_{-1.63}) \times 10^3$
$T_{4c}^{0^{++}} \rightarrow \text{LH}$	37 ± 26	$(3.80 \pm 2.67^{+6.37}_{-2.03}) \times 10^6$	9 ± 6	$(0.96 \pm 0.64^{+1.60}_{-0.51}) \times 10^5$
$T_{4c}^{2^{++}} \rightarrow \text{LH}$	93 ± 65	$(5.94 \pm 4.15^{+9.95}_{-3.17}) \times 10^6$	81 ± 57	$(4.52 \pm 3.18^{+7.58}_{-2.42}) \times 10^6$

inside the tetraquark, and the subscript ‘‘Coulomb’’ indicates that the LDME is evaluated using the diquark model with the interquark and interdiquark potentials being Coulombic. By taking $m_b = 4.8 \text{ GeV}$, $v_b = \sqrt{0.1}$, $v_c = \sqrt{0.3}$, and $\alpha_s(2m_b) = 0.175$, we predict $\Gamma[T_{4b}^{0^{++}} \rightarrow \gamma\gamma] = (1.4\text{--}4.1) \times 10^{-7} \text{ MeV}$, $\Gamma[T_{4b}^{2^{++}} \rightarrow \gamma\gamma] = (0.6\text{--}0.7) \times 10^{-7} \text{ MeV}$, $\Gamma[T_{4b}^{0^{++}} \rightarrow \text{LH}] = (0.9\text{--}8.6) \times 10^{-4} \text{ MeV}$, and $\Gamma[T_{4b}^{2^{++}} \rightarrow \text{LH}] = (4.6\text{--}5.4) \times 10^{-4} \text{ MeV}$. We find the decay width of $T_{4b} \rightarrow \gamma\gamma$ is roughly 3 orders of magnitude smaller than that of T_{4c} , while the decay width of $T_{4b} \rightarrow \text{LH}$ is 2 orders of magnitude smaller than the T_{4c} counterpart.

Combining our predictions with the T_{4c} production cross sections at the LHC [47], we can further estimate the event yields for the T_{4c} hadronic and electromagnetic decay at the LHC. The event numbers for various channels are tabulated in Table III. For reference, we also copy the T_{4c} cross sections from Ref. [47] in the table. It is expected that there will be plenty of $T_{4c} \rightarrow \text{LH}$ signals accumulated at the LHC. In spite of potentially copious background events, it seems that the observation prospects for the T_{4c} hadronic decay are promising. On the other hand, the event numbers for the electromagnetic decay $T_{4c} \rightarrow \gamma\gamma$ are much smaller; nevertheless, it is hopeful to probe these channels, thanks to a clean final state topology in which the diphoton invariant mass can be reconstructed with high precision.

V. SUMMARY

By applying the NRQCD factorization formalism, we compute the decay widths for the S-wave fully heavy tetraquark T_{4Q} hadronic as well as electromagnetic decay at lowest order in α_s and v . The SDCs are determined through the procedure of perturbative matching. The LDMEs are

related to the phenomenological four-body Schrödinger wave functions at the origin, whose values are taken from Refs. [22,35]. To obtain the branching fractions for T_{4c} decay, we approximate the total decay width of T_{4c} with $\Gamma[T_{4c} \rightarrow J/\psi J/\psi]$. The latter value has been determined by the LHCb, CMS, and ATLAS Collaborations. We find the branching fractions are around 10^{-3} and 10^{-6} for the T_{4c} hadronic decay and electromagnetic decay, respectively. It is worth noting that the branching fractions for $T_{4c}^{2^{++}}$ are insensitive to the phenomenological models, while the predictions for $T_{4c}^{0^{++}}$ from Ref. [22] are more than 2 times larger than these from Ref. [35]. This feature is quite similar to the case for the T_{4c} production at the LHC. Combining the T_{4c} production cross sections with the branching fractions for T_{4c} decay, we estimate the event numbers for various decay channels at the LHC. The observation prospect seems to be promising for both the T_{4c} hadronic and electromagnetic decay.

ACKNOWLEDGMENTS

The work of W.-L. S. and T. W. is supported by the National Natural Science Foundation of China under Grants No. 12375079 and No. 11975187, and the Natural Science Foundation of ChongQing under Grant No. CSTB2023NSCQ-MSX0132. The work of Y.-D. Z. is supported by the National Natural Science Foundation of China under Grants No. 12135006 and No. 12075097, as well as by the Fundamental Research Funds for the Central Universities under Grants No. CCNU20TS007 and No. CCNU22LJ004. The work of F. F. is supported by the National Natural Science Foundation of China under Grants No. 12275353 and No. 11875318.

- [1] R. Aaij *et al.* (LHCb Collaboration), *Sci. Bull.* **65**, 1983 (2020).
- [2] J. Zhang *et al.* (CMS Collaboration), *Proc. Sci. ICHEP2022* 775.
- [3] A. Hayrapetyan *et al.* (CMS Collaboration), *arXiv:2306.07164*.
- [4] Kai Yi (on behalf of the CMS Collaboration), Recent CMS results on exotic resonance, *Proceedings at ICHEP* (2022), <https://agenda.infn.it/event/28874/contributions/170300/>.
- [5] Y. Xu (ATLAS Collaboration), *Acta Phys. Pol. B Proc. Suppl.* **16**, 21 (2023).
- [6] E. B.-T. (on behalf of the ATLAS Collaboration), <https://agenda.infn.it/event/28874/contributions/170298/>.
- [7] V. Khachatryan *et al.* (CMS Collaboration), *J. High Energy Phys.* **05** (2017) 013.
- [8] A. M. Sirunyan *et al.* (CMS Collaboration), *Phys. Lett. B* **808**, 135578 (2020).
- [9] R. Aaij *et al.* (LHCb Collaboration), *J. High Energy Phys.* **10** (2018) 086.
- [10] Y. Iwasaki, *Phys. Rev. Lett.* **36**, 1266 (1976).
- [11] K. T. Chao, *Z. Phys. C* **7**, 317 (1981).
- [12] J. P. Ader, J. M. Richard, and P. Taxil, *Phys. Rev. D* **25**, 2370 (1982).
- [13] A. M. Badalian, B. L. Ioffe, and A. V. Smilga, *Nucl. Phys.* **B281**, 85 (1987).
- [14] A. V. Berezhnuy, A. V. Luchinsky, and A. A. Novoselov, *Phys. Rev. D* **86**, 034004 (2012).
- [15] J. Wu, Y. R. Liu, K. Chen, X. Liu, and S. L. Zhu, *Phys. Rev. D* **97**, 094015 (2018).
- [16] N. Barnea, J. Vijande, and A. Valcarce, *Phys. Rev. D* **73**, 054004 (2006).
- [17] M. S. Liu, Q. F. Lü, X. H. Zhong, and Q. Zhao, *Phys. Rev. D* **100**, 016006 (2019).
- [18] G. J. Wang, L. Meng, and S. L. Zhu, *Phys. Rev. D* **100**, 096013 (2019).
- [19] M. A. Bedolla, J. Ferretti, C. D. Roberts, and E. Santopinto, *Eur. Phys. J. C* **80**, 1004 (2020).
- [20] C. Deng, H. Chen, and J. Ping, *Phys. Rev. D* **103**, 014001 (2021).
- [21] X. Jin, Y. Xue, H. Huang, and J. Ping, *Eur. Phys. J. C* **80**, 1083 (2020).
- [22] Q. F. Lü, D. Y. Chen, and Y. B. Dong, *Eur. Phys. J. C* **80**, 871 (2020).
- [23] J. Zhang, J. B. Wang, G. Li, C. S. An, C. R. Deng, and J. J. Xie, *Eur. Phys. J. C* **82**, 1126 (2022).
- [24] Z. G. Wang, *Eur. Phys. J. C* **77**, 432 (2017).
- [25] W. Chen, H. X. Chen, X. Liu, T. G. Steele, and S. L. Zhu, *Phys. Lett. B* **773**, 247 (2017).
- [26] Z. G. Wang, *Chin. Phys. C* **44**, 113106 (2020).
- [27] R. H. Wu, Y. S. Zuo, C. Y. Wang, C. Meng, Y. Q. Ma, and K. T. Chao, *J. High Energy Phys.* **11** (2022) 023.
- [28] Y. Bai, S. Lu, and J. Osborne, *Phys. Lett. B* **798**, 134930 (2019).
- [29] M. C. Gordillo, F. De Soto, and J. Segovia, *Phys. Rev. D* **102**, 114007 (2020).
- [30] C. Hughes, E. Eichten, and C. T. H. Davies, *Phys. Rev. D* **97**, 054505 (2018).
- [31] Z. R. Liang, X. Y. Wu, and D. L. Yao, *Phys. Rev. D* **104**, 034034 (2021).
- [32] F. Carvalho, E. R. Cazaroto, V. P. Gonçalves, and F. S. Navarra, *Phys. Rev. D* **93**, 034004 (2016).
- [33] R. Maciula, W. Schäfer, and A. Szczurek, *Phys. Lett. B* **812**, 136010 (2021).
- [34] H. X. Chen, W. Chen, X. Liu, and S. L. Zhu, *Sci. Bull.* **65**, 1994 (2020).
- [35] M. S. Liu, F. X. Liu, X. H. Zhong, and Q. Zhao, *arXiv:2006.11952*.
- [36] J. F. Giron and R. F. Lebed, *Phys. Rev. D* **102**, 074003 (2020).
- [37] M. Karliner and J. L. Rosner, *Phys. Rev. D* **102**, 114039 (2020).
- [38] R. M. Albuquerque, S. Narison, A. Rabemananjara, D. Rabetiarivony, and G. Randriamanatrika, *Phys. Rev. D* **102**, 094001 (2020).
- [39] B. D. Wan and C. F. Qiao, *Phys. Lett. B* **817**, 136339 (2021).
- [40] X. K. Dong, V. Baru, F. K. Guo, C. Hanhart, and A. Nefediev, *Phys. Rev. Lett.* **126**, 132001 (2021); **127**, 119901(E) (2021).
- [41] Z. H. Guo and J. A. Oller, *Phys. Rev. D* **103**, 034024 (2021).
- [42] H. X. Chen, W. Chen, X. Liu, Y. R. Liu, and S. L. Zhu, *Rep. Prog. Phys.* **86**, 026201 (2023).
- [43] F. Feng, Y. Huang, Y. Jia, W. L. Sang, X. Xiong, and J. Y. Zhang, *Phys. Rev. D* **106**, 114029 (2022).
- [44] G. T. Bodwin, E. Braaten, and G. P. Lepage, *Phys. Rev. D* **51**, 1125 (1995); G. T. Bodwin, E. Braaten, and G. P. Lepage, *Phys. Rev. D* **55**, 5853(E) (1997).
- [45] Y. Q. Ma and H. F. Zhang, *arXiv:2009.08376*.
- [46] R. Zhu, *Nucl. Phys.* **B966**, 115393 (2021).
- [47] F. Feng, Y. Huang, Y. Jia, W. L. Sang, D. S. Yang, and J. Y. Zhang, *Phys. Rev. D* **108**, L051501 (2023).
- [48] F. Feng, Y. Huang, Y. Jia, W. L. Sang, and J. Y. Zhang, *Phys. Lett. B* **818**, 136368 (2021).
- [49] Y. Huang, F. Feng, Y. Jia, W. L. Sang, D. S. Yang, and J. Y. Zhang, *Chin. Phys. C* **45**, 093101 (2021).
- [50] T. Hahn, *Comput. Phys. Commun.* **140**, 418 (2001).
- [51] R. Mertig, M. Bohm, and A. Denner, *Comput. Phys. Commun.* **64**, 345 (1991).
- [52] F. Feng and R. Mertig, *arXiv:1212.3522*.
- [53] J. Kuipers, T. Ueda, J. A. M. Vermaseren, and J. Vollinga, *Comput. Phys. Commun.* **184**, 1453 (2013).
- [54] K. G. Chetyrkin, J. H. Kuhn, and M. Steinhauser, *Comput. Phys. Commun.* **133**, 43 (2000).
- [55] V. Biloshytskyi, L. Harland-Lang, B. Malaescu, V. Pascalutsa, K. Schmieden, and M. Schott, *EPJ Web Conf.* **274**, 06007 (2022).